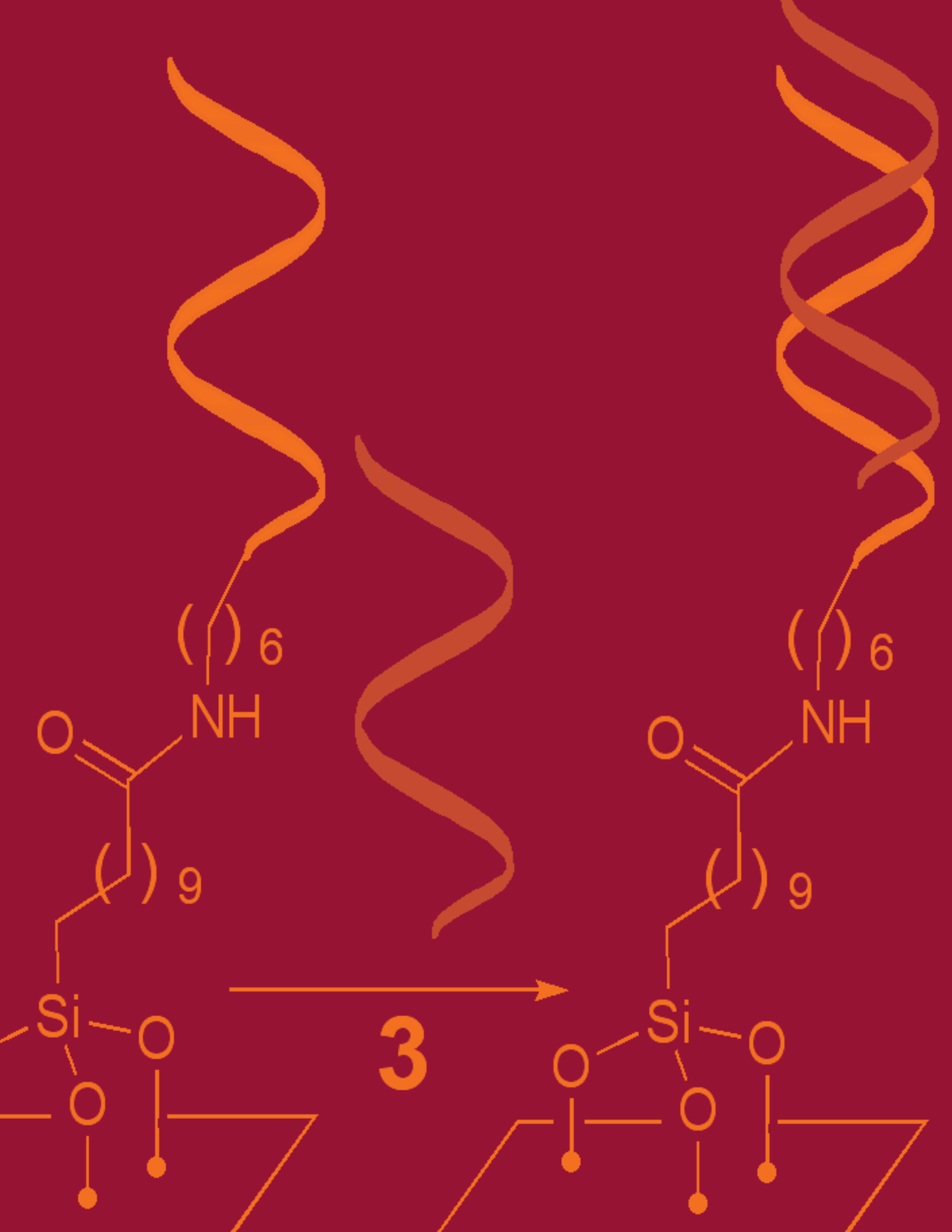
( )6
NH
O
( )9
Si
O
O
3
( )6
NH
O
( )9
Si
O
O
O

DNA Surface Characterization Using Second Harmonic Generation and Contact-Angle Goniometry

Undergraduate Researcher
Boyee Wong
California Polytechnic State University,
San Luis Obispo

Faculty Mentor
Franz Geiger
Department of Chemistry
Northwestern University

Graduate Student Mentor
Faith Boman
Department of Chemistry
Northwestern University

Abstract

Chip-based devices and biosensors incorporate the attachment of biomolecules at interfaces. The behavior of biomolecules at the surface and interfaces differs from the behavior of biomolecules in the bulk solution. Surface-analysis techniques are therefore required to characterize these interfaces. Second harmonic generation (SHG) has been used to characterize DNA on a quartz lens to model biomolecules at the surface. Optimization of the surface-attachment procedure using contact-angle goniometry is necessary to optimize the results of laser experiments. Contact-angle goniometry is used to optimize surface preparation parameters, such as concentration of NHS, concentration of water, reaction time, and various cleaning strategies. Studying DNA surfaces can assist with improvements in DNA detection systems for biodiagnostics by determining important structural information about the biomolecules.

Introduction

Nanotechnology uses nanoscale devices such as biosensors and biochips in the study of biodiagnostics and disease prevention.[1–4] The design of these chip-based surfaces involves the attachment of biomolecules to an interface, thus allowing the surface-bound molecules to interact with biomolecules in solution. Although biomolecules have been studied a great deal in bulk solution, they may behave differently at an interface.[5,6] Because interfaces have not been as well characterized, it is necessary to apply surface-analysis techniques to assess differences between bulk and interfacial behavior and to study these interfaces. Advancing biodetection approaches requires gaining molecular-level insight into biomolecules at the interface.[2,7,8]

Many surface-analysis techniques such as atomic force microscopy,[9] colorimetry,[4,10] Fourier transform infrared spectroscopy,[11] surface plasmon resonance spectroscopy,[12,13] fluorescence spectroscopy[14] and electrochemistry[15] have been used to characterize DNA-functionalized surfaces of interfaces. SHG, a powerful surface-specific optical technique,[6] can be used to investigate these systems on a molecular level.

Recently, SHG has been used to study the DNA-fused-quartz functionalized interface.[16,17] In order to obtain reproducible and reliable results in the laser experiments, the reaction conditions under which the DNA and the linker are attached to the surface must be standardized. Parameters such as reactant concentrations, cleaning methods, and reaction time are optimized through contact-angle goniometry to improve the surface preparation. By studying DNA surfaces, important structural information can be determined about the biomolecules that will help to assist in the design improvements of DNA detection systems for biodiagnostics and early treatment of disease.[13,16,18–20]

Background

Contact-angle goniometry is useful for characterizing a variety of surfaces that undergo chemical change. It is a surface-analysis technique that measures the angle formed by the curvature of a water droplet on a solid surface (see Figure 2B). Analysis of these angles yields the surface tension and interfacial energy of a sessile water droplet on a surface.[21] In a wetting experiment, a syringe is used to bring microliter aliquots of a test liquid into contact with the surface, and a camera captures the profile of the droplet. Software automatically calculates the angle between the tangent of the droplet and the solid. This automatic analysis reduces the error involved with manual measurements, thus increasing consistency.

Contact-angle measurements are a simple way to quantify surface wetability and provide insight into the energetics of the surface structure.[21] The curvature of the droplet is related to the hydrophobicity of the surface. Since water is a polar liquid, a water droplet resists contact with a nonpolar (hydrophobic) surface, resulting in a large contact angle. A polar surface, in contrast, is hydrophilic, causing a water droplet to favorably interact with the surface and spread. The result is a contact angle closer to 0°.

A variety of surfaces have been characterized by contact-angle goniometry, such as acetylenyl-terminated self-assembled monolayers on gold,[22] titanium(IV)

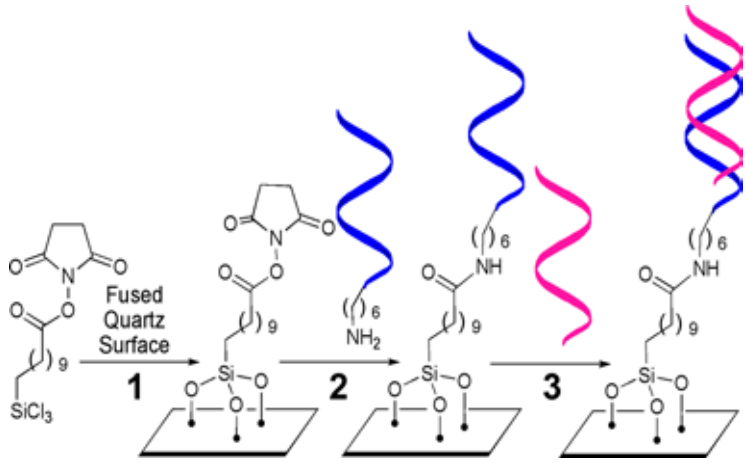

Figure 1. Surface preparation of DNA-functionalized interfaces. Step 1 depicts the attachment of the *N*-hydroxysuccinimidyl (NHS) ester-terminated siloxane on fused quartz. Step 2 depicts the coupling of the 3'-amine-terminated DNA strand to the NHS linker. Step 3 depicts the hybridization of the complementary DNA strand to surface-bound DNA.

alkoxides on functionalized gold surfaces,[23] and flax fibers.[24] Contact-angle measurements are useful in tracking the progress of a reaction in which the hydrophobicity of the surface is modified. Previously studied reactions include the acylation of grafting architectures on ethylene-acrylic acid copolymer films[25] and the irradiation of polytetrafluoroethylene films.[26] Since contact-angle measurements provide a measure of the relative hydrophobicity of a surface, goniometry is an advantageous method to characterize the reaction steps involved in binding short strands of DNA to a polar- fused quartz surface via a nonpolar linker.

SHG is a surface-specific, nonlinear optical phenomenon that only occurs where centrosymmetry is broken, such as at an interface.[5,6,18,27,28] In SHG, two incident photons with a given frequency are combined to create one photon with double the frequency and half the initial wavelength.[29]

SHG does not require the use of labels to measure changes associated with surface-bound DNA. Labels are not necessary because, in the application of SHG to label-free DNA-functionalized interfaces, the signal originates from either the charged backbone, the molecular chirality of the duplex or electronic resonances of the bases.[16,17] This is an advantage over many other surface-characterization techniques that require labeling, such as fluorescence, nanoparticle tagging, electrochemistry, and radioactivity. Eliminating the use of labels simplifies DNA sample preparation and causes the signal to a directly result from the studied molecule. This makes SHG a very powerful and versatile technique to study DNA at an interface in situ and in real time.

There is much interest in SHG due to its high sensitivity and surface specificity.[5] It has been used to study single crystals,[30] metals,[31] thin films,[32] adsorbed monolayers,[33] liposome bilayers,[34] and functionalized organic monolayers.[35] It has also been used to determine surface pK_a,[36,37] adsorption kinetics,[38–40] surface symmetry, molecular orientation,[32,41,42] and chirality.[32,43,44] SHG has recently been applied to study DNA-functionalized interfaces,[16,17] and this field is the focus of this paper.

Approach

In order to study DNA-functionalized interfaces by SHG, the sample surface needs preparing before chemically attaching the short strands of DNA via a linker (Figure 1). Reproducible results with consistently high surface coverages made under well-defined reaction conditions are necessary for accurate SHG laser experiments. The reaction process must therefore be standardized.

Samples were prepared by exposing clean glass microscope slides to a nonpolar *N*-hydroxysuccinimidyl (NHS) linker dissolved in toluene with a small quantity of water. The slides were originally prepared in a solution with toluene, 1.4 mM NHS, and 0.1%v/v water, and reacted overnight. To determine optimal reaction conditions, several series of samples were prepared varying one parameter — water concentration, NHS concentration and reaction time — at a time.

A second investigation was performed to determine the best method for cleaning the slides once they were exposed to NHS. The samples for the laser experiments are expensive, so it is necessary to reuse the samples and ensure their cleanliness. The contact angle of the

NHS adlayer on each sample slide was analyzed with a First Ten Angstroms (FTA-100 series) goniometer and drop-analysis software. After the functionalized surfaces were studied, they were exposed to Nochromix® (Godax Laboratories, Inc.), a strong glass-cleaning reagent, sonicated in methanol, and plasma-cleaned. The exposure time to Nochromix was varied to assess the length of time necessary for the surface to be thoroughly cleaned. Some surfaces were sonicated and plasma-cleaned to test whether Nochromix was necessary in the cleaning process.

The samples for the SHG laser experiments were hemispherical, fused quartz lenses reacted with NHS in the same way as the glass slide samples. Short strands of amine-terminated DNA (15–35 thymidine base pairs) dissolved in a sodium tetraborate buffer ($Na_2B_4O_7$) solution were reacted for 4 hr with the linker surfaces. The samples were probed in a sample cell under aqueous conditions. An optical parametric amplifier (OPA-800CF, Spectra-Physics Lasers) pumped by a Ti:Sapphire laser (800 nm, 120 fs, kHz repetition rate, Hurricane, Spectra-Physics) was tuned to the desired frequency and directed onto the sample through a series of optics, including filters, a half-waveplate, and a focusing lens. The second harmonic signal generated at the interface was focused through a monochromator and into a photomultiplier tube, where it was collected using single-photon counting techniques. The input frequency was filtered beforehand using appropriate filters (Kopp Glass #9863 and #5840). Control experiments were performed to test for generation of SH signal and proper alignment of optics.

Results and Discussion

Contact angles of a sessile drop of water on a clean glass microscope slide and on an NHS-functionalized glass slide (Figure 2) were calculated to be 6° and 54(4)°, respectively. The glass slide is hydrophilic, and the contact angle is therefore low. The NHS surface is more hydrophobic, which causes the droplet to bead up on the surface and create a larger contact angle. The reaction progress was quantified by measuring the contact angles as various reaction parameters were changed. Table 1 summarizes the experiments performed by changing the concentration of linker, the concentration of water, and the reaction time of the deposition. An average of 12 to 15 drops were measured on each sample, with two to four samples for each experiment.

The first parameter tested was the water concentration (Figure 3). The linker was nonpolar and dissolved in toluene, but a small quantity of water is necessary for the reaction on the surface to proceed. If there is too much water in the toluene, the linker will polymerize. The linker was air-sensitive and kept in a glove box filled with nitrogen prior to its use. The range of concentrations for water dissolved in the toluene was 0.01% to 1% v/v. The values of the contact angle were all within error of one another. There was no significant change in the contact angles for the different water concentrations. This indicated a large degree of flexibility in this variable.

The NHS concentration was also varied; the results of the contact-angle measurements are shown in Figure 4. The linker was synthesized in limited quantities. The concentration range tested was 1.4 to 5.6 mM, and the contact angles slightly changed in this range. This suggested that

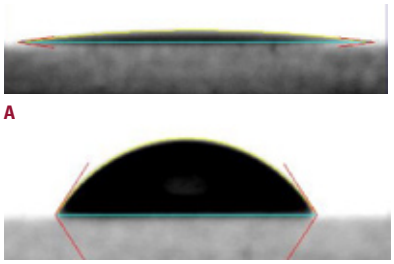

A

B

Figure 2. Contact angle of a sessile drop of water on a (A) clean glass microscope slide and an (B) NHS-functionalized glass slide. The contact angles of slides A and B are 6° and 54(4)°, respectively.

[H_2O] [%v/v]	[Linker] [mM]	Time [hr]	Contact Angle [o]
0.01	1.4	6	55(4)
0.1	1.4	6	54(4)
0.2	0.7	6	61(4)
0.5	0.3	6	55(8)
1	0.1	6	57(5)
0.1	1.4	6	54(2)
0.1	2.9	6	52(2)
0.1	5.7	6	54(4)
0.1	1.4	1	57(2)
0.1	1.4	4	57(3)
0.1	1.4	6	54(2)
0.1	1.4	8	58(3)
0.1	1.4	12	53(7)
0.1	1.4	24	58(5)

Table 1. Average contact angles of NHS slides.

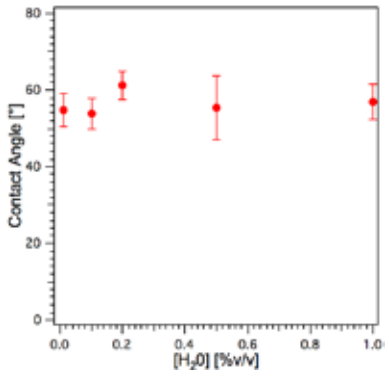

Figure 3. Contact angles of NHS slides as a function of water concentration. The contact angle is constant within error.

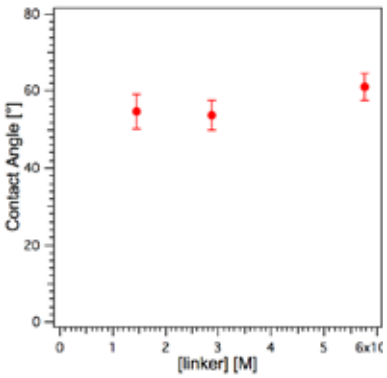

Figure 4. Contact angles of the NHS slides as a function of linker concentration. The contact angle is constant within error.

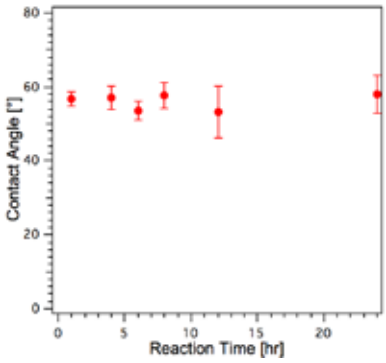

Figure 5. Contact angles of the NHS slides as a function of reaction time. The contact angle is constant within error.

Figure 6. Sessile drop of water on a glass microscope slide that has been cleaned with Nochromix for 1 hr, sonicated in methanol for 15 min, and plasma-cleaned in O_2 for 30 sec. The contact angle is 4°, indicating a clean and hydrophilic surface.

it was unnecessary to use a higher concentration of NHS, since it does not result in a detectably higher surface coverage. Instead, it was reasonable to test whether a lower concentration of NHS can be used to produce the same results.

The contact-angle measurements as a function of reaction time are shown in Figure 5. The contact angle did not change as a function of linker deposition time, but the error associated with these measurements increased. These measurements indicated that it is reasonable to allow the reaction to proceed for 4 to 6 hr instead of overnight, and that the reaction occurs relatively quickly compared with what was previously expected. Combining the above results, it was observed that the optimal conditions include: solution of 0.1% v/v water, 1.4 mM NHS, and a 4-6 hr reaction time.

Two cleaning strategies were employed and compared. One set of NHS-coated surfaces was cleaned in the Nochromix, sonicated, and plasma-cleaned. Another set of surfaces was only sonicated and plasma-cleaned. Figure 6 shows a functionalized slide cleaned with Nochromix and illustrated that the first cleaning method (with Nochromix) produced a more hydrophilic surface. With this method, the droplet spread over a wider range, producing a lower contact angle. Figure 7 shows the results of cleaning the slides that were previously reacted (Figure 5) and cleaned with Nochromix for varying times. The contact angles were two to three degrees lower than the surfaces not treated with Nochromix. This indicated that Nochromix cleaned the surface more effectively and brought the surface back to its original condition. These surfaces

can be reused for future reactions. New slides will be precleaned with Nochromix for future experiments.

The Gaussian profile of the generated second harmonic signal at 267.5 nm from femtosecond pulses on an ssDNA T_{35}-mer functionalized lens is shown in Figure 8. The UV-Vis spectrum of the input Gaussian beam at 536 nm is shown in the inset. The output profile was captured by changing the monochromator setting. This control study verifies the observation of a second harmonic signal at double the frequency of the probe beam.

Another control study was performed to rotate an input polarization while collecting the output polarizations. The polarization-controlled response of the sample has implications in chirality and molecular orientation.[16,17] In Figure 9, a clean fused-quartz lens was probed with an input wavelength of 530 nm at 0.5 µJ. In Figure 10, the NHS-functionalized fused-quartz lens was probed with an input wavelength of 536 nm at 0.5 µJ. A half-waveplate was used to change the input polarization angles, altering the orientation of the light directed on the surface. The maxima and periodic pattern indicate that the sample cell is well aligned, which is important for future chiral laser work on DNA.

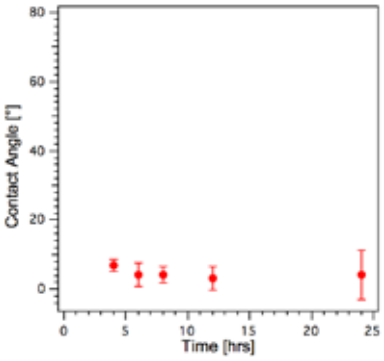

Figure 7. Contact angles of the NHS slides shown in Figure 5 after being cleaned with Nochromix, sonicated, and plasma-cleaned. The angles indicate that Nochromix is effective in cleaning adlayers from slides that have undergone a range of reaction times.

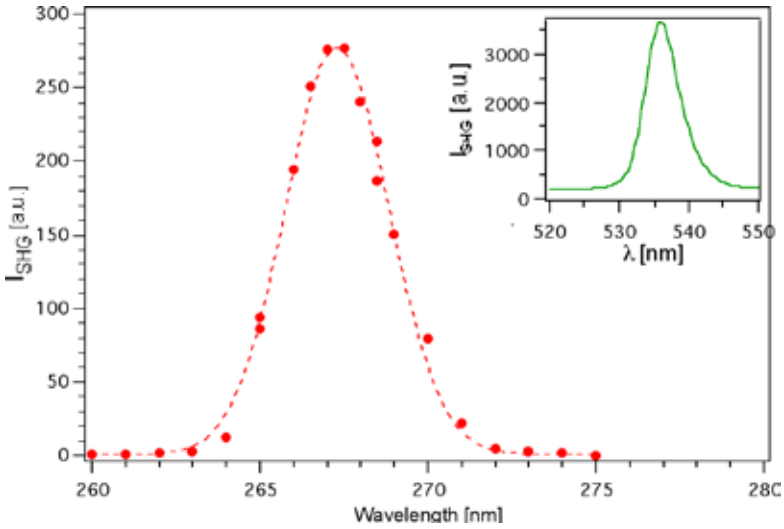

Figure 8. Monochromator output from femtosecond pulses shows a Gaussian profile. The dashed line is a fit of the Gaussian function. The sample is a ssDNA T_{35}-functionalized fused-quartz lens. The input laser frequency is 536 nm, the output frequency is 267.5 nm, and the power is 0.5 µJ. Inset: UV-Vis spectrum of the input wavelength.

Conclusion

To improve nano-biodiagnostic devices, it is necessary to gain a complete understanding of the interfaces between molecules. In this research biomolecules were modeled with DNA functionalized on the surface. The optimal surface preparation conditions were determined by using contact-angle measurements and included variations of the NHS-linker concentration, water concentra-

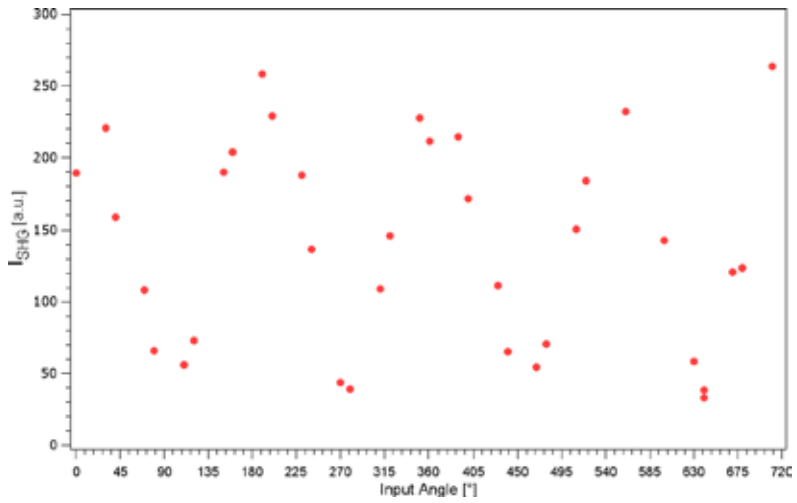

Figure 9. Periodic response in signal as a function of input polarization. The sample is a clean fused-quartz lens. The input laser frequency is 530 nm, and the power is 0.5 µJ. The polarization is controlled by a half-waveplate. The symmetric and periodic signal intensity indicates that the optics are well aligned.

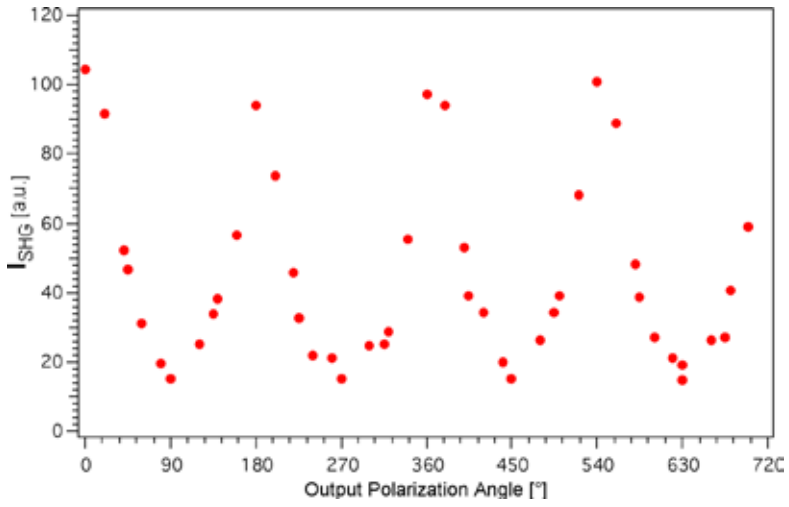

Figure 10. Periodic response in signal as a function of input polarization. The sample is an NHS-functionalized fused-quartz lens. The input laser frequency is 530 nm, and the power is 0.5 µJ. The polarization is controlled by a half-waveplate. The symmetric and periodic signal intensity indicates that the optics are well aligned.

tion, and length of reaction time. It was found that the optimal reaction solution consists of a NHS-linker concentration of 1.4 mM, a water concentration of 0.1% v/v, and a reaction time of 4 to 6 hr. In addition, the surfaces should be exposed to Nochromix, sonicated in methanol, and plasma-cleaned prior to use. Control studies confirmed that the system was generating a second harmonic signal and also demonstrating well-aligned optics.

This research was supported primarily by the Nanoscale Science and Engineering Initiative of the National Science Foundation under NSF Award Number ***EEC-0647560.*** *Any opinions, findings and conclusions or recommendations expressed in this material are those of the author(s) and do not necessarily reflect those of the National Science Foundation.*

References

(1) Niemeyer, C. M.; Burger, W.; Peplies, J. *Angew. Chem., Int. Ed. Engl.* **1998**, *37*, 2265–2268.

(2) Arlinghaus, H. F.; Kwoka, M. N.; Jacobson, K. B. *Anal. Chem.* **1997**, *69*, 3747–3753.

(3) Whaley, S. R.; English, D. S.; Hu, E. L.; Barbara, P. F.; Belcher, A. M. *Nature* **2000**, *405*, 665–668.

(4) Elghanian, R.; Storhoff, J. J.; Mucic, R. C.; Letsinger, R. L.; Mirkin, C. A. *Science* **1997**, *277*, 1078–1080.

(5) Shen, Y. R. *Nature* **1989**, *337*, 519–525.

(6) Simpson, G. J. Appl. *Spectrosc.* **2001**, *55*, 16A–32A.

(7) Mirkin, C. A.; Taton, T. A. *Nature* **2000,** *405,* 626–627.

(8) Mirkin, C. A.; Letsinger, R. L.; Mucic, R. C.; Storhoff, J. J. *Nature* **1996,** *382,* 607–609.

(9) Wang, J.; Bard, A. J. *Anal. Chem.* **2001,** *73,* 2207–2212.

(10) Taton, T. A.; Mirkin, C. A.; Letsinger, R. L. *Science* **2000,** *289,* 1757–1760.

(11) Boncheva, M.; Scheibler, L.; Lincoln, P.; Vogel, H.; Aakerman, B., *Langmuir* **1999,** *15,* 4317–4320.

(12) Georgiadis, R.; Peterlinz, K. P.; Peterson, A. W., J. *Am. Chem. Soc.* **2000,** *122,* 3166–3173.

(13) Nelson, B. P.; Grimsrud, T. E.; Liles, M. R.; Goodman, R. M.; Corn, R. M., *Anal. Chem.* **2001,** *73,* 1–7.

(14) Strother, T.; Cai, W.; Zhao, X.; Hamers, R. J.; Smith, L. M., J. Am. *Chem. Soc.* **2000,** *122,* 1205–1209.

(15) Finot, E.; Bourillot, E.; Meunier-Prest, R.; Lacroute, Y.; Legay, G.; Cherkaoui-Malki, M.; Latruffe, N.; Siri, O.; Braunstein, P.; Dereux, A., *Ultramicroscopy* **2003,** *97,* 441–449.

(16) Boman, F. C.; Musorrafiti, M. J.; Gibbs, J. M.; Stepp, B. R.; Salazar, A. M.; Nguyen SonBinh, T.; Geiger, F. M. J. *Am. Chem. Soc.* **2005,** *127,* 15368–15369.

(17) Stokes, G. Y.; Gibbs-Davis, J. M.; Boman, F. C.; Stepp, B. R.; Condie, A. G.; Nguyen, S. T.; Geiger, F. M. J. *Am. Chem. Soc.* **2007,** *129,* 7492–7493.

(18) Shen, Y. R. J. *Vac. Sci. Technol. B* **1985,** *3,* 1464–1466.

(19) Huang, E.; Zhou, F.; Deng, L. *Langmuir* **2000,** *16,* 3272–3280.

(20) Silverman, A. P.; Kool, E. T. *Chem. Rev.* **2006,** *106,* 3775–3789.

(21) *In Contact Angle, Wettability, and Adhesion,* Kendall Award Symposium, Los Angeles, CA, April 2-3, 1963; Fowkes, F. M., Ed. American Chemical Society: Los Angeles, CA, 1963; p 389.

(22) Lee, J. K.; Chi, Y. S.; Choi, I. S. *Langmuir* **2004,** *20,* 3844–3847.

(23) Banks, J. T.; Yu, T. T.; Yu, H. Z. J. *Phys. Chem. B* **2002,** *106,* 3538–3542.

(24) Zini, E.; Scandola, M.; Gatenholm, P. *Biomacromolecules* **2003,** *4,* 821–827.

(25) Janorkar, A. V.; Luo, N.; Hirt, D. E. *Langmuir* **2004,** *20,* 7151–7158.

(26) Hopp, B.; Kresz, N.; Kokavecz, J.; Smausz, T.; Schieferdecker, H.; Doring, A.; Marti, O.; Bor, Z. *Appl. Surf. Sci.* **2004,** *221,* 437–443.

(27) Boyd, R. W., *Nonlinear Optics.* 2nd ed.; Acaemic Press: New York, 2003; p 578.

(28) Shen, Y. R., *The Principles of Nonlinear Optics;* John Wiley & Sons, Inc: New York, 2003; p 563.

(29) Corn, R. M.; Higgins, D. A. *Chem. Rev.* **1994,** *94,* 107–125.

(30) Fitts, J. P.; Shang, X.; Flynn, G. W.; Heinz, T. F.; Eisenthal, K. B. J. *Phys. Chem. B* **2005,** *109,* 7981–7986.

(31) Tom, H. W. K.; Mate, C. M.; Zhu, X. D.; Crowell, J. E.; Heinz, T. F.; Somorjai, G. A.; Shen, Y. R. *Phys. Rev. Lett.* **1984,** *52,* 348.

(32) Simpson, G. J. *ChemPhysChem* **2004,** *5,* 1301–1310.

(33) Han, S. H.; Ji, N.; Belkin, M. A.; Shen, Y. R. *Phys. Rev. B* **2002,** *66,* 165415/1–165415/6.

(34) Shang, X.; Liu, Y.; Yan, E.; Eisenthal, K. B. *J. Phys. Chem. B* **2001,** *105,* 12816–12822.

(35) Al-Abadleh, H. A.; Mifflin, A. L.; Bertin, P. A.; Nguyen, S. T.; Geiger, F. M. *J. Phys. Chem. B* **2005,** *109,* 9691–9702.

(36) Zhao, X.; Ong, S.; Wang, H.; Eisenthal, K. B. *Chem. Phys. Lett.* **1993,** *214,* 203–207.

(37) Konek, C. T.; Musorrafiti, M. J.; Al-Abadleh, H. A.; Bertin, P. A.; Nguyen, S. T.; Geiger, F. M. *J. Am. Chem. Soc.* **2004,** *126,* 11754–11755.

(38) Mifflin, A. L.; Gerth, K. A.; Geiger, F. M. *J. Phys. Chem. A* **2003***, 107,* 9620–9627.

(39) Al-Abadleh, H. A.; Voges, A. B.; Bertin, P. A.; Nguyen, S. T.; Geiger, F. M. *J. Am. Chem. Soc.* **2004,** *126,* 11126–11127.

(40) Al-Abadleh, H. A.; Mifflin, A. L.; Musorrafiti, M. J.; Geiger, F. M. *J. Phys. Chem. B* **2005,** *109,* 16852–16859.

(41) Miranda, P. B.; Pflumio, V.; Saijo, H.; Shen, Y. R. *Chem. Phys. Lett.* **1997,** *264,* 387–392.

(42) Salafsky, J. S.; Eisenthal, K. B. *Chem. Phys. Lett.* **2000,** *319,* 435–439.

(43) Hicks, J. M.; Kemnitz, K.; Eisenthal, K. B.; Heinz, T. F. *J. Phys. Chem.* **1986,** *90,* 560–562.

(44) Ji, N.; Shen, Y.-R. *J. Am. Chem. Soc.* **2004,** *126,* 15008–15009.